DETERMINATION OF THE SHAPE AND DURATION OF PICOSECOND LIGHT PULSES BY BLEACHING OF DYES

J. WIEDMANN and A. PENZKOFER

Fachbereich Physik der Universität Regensburg,
8400 Regensburg, Germany

A new method is developed to measure the shape and duration of picosecond light pulses in a single shot. A pump and probe technique in a dye sample is applied. Single picosecond light pulses at different frequencies were analysed with various absorbers. Asymmetric pulse shapes with leading edges steeper than the trailing edges were observed.

1. Introduction

The knowledge of the duration and shape of picosecond light pulses is essential in time resolved picosecond studies. Various techniques for the measurement of picosecond pulse durations are summarized in recent reviews [1,2,3]. The most widely used methods are the two-photon-fluorescence technique (TPF) [4], the non-collinearly phasematched second harmonic generation (SHG) [5], the Kerr shutter technique [6], and streak camera measurements [7]. Autocorrelation measurements with TPF, SHG and Kerr shutter method give no information on the symmetry of the pulse shape. Streak cameras with high temporal resolution may be used for pulse shape determinations. A few measurements of the time profile of picosecond light pulses applying different techniques have been reported [8–12].

In this paper we describe a new pump and probe technique which applies bleaching dyes and gives the temporal shape and duration of single picosecond light pulses in single shots.

2. Theory

The basic principle of the new technique is schematically shown in fig. 1. An intense pump pulse approaches the absorber cell from the left and excites
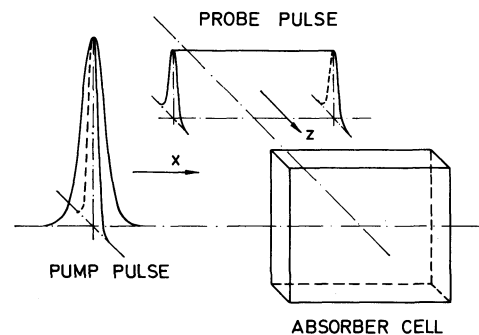

Fig. 1. Basic principle of pulse shape measurement. An intense pump pulse bleaches the absorber in the cell. The probe beam interrogates with the travelling transmission front in the sample. The spatial derivative $\partial T_E / \partial x$ of the time integrated transmission of the probe pulse is proportional to the incident time shape of the probe beam.

the dye. An excitation front is built up and travels approximately with ligh velocity through the dye sample. The excitation causes an increase in transmission. An expanded probe beam is passed perpendicular to the pump pulse through the sample and interrogates with the transmission front. In the overlapping range the transmission of the probe beam changes from strong absorption at the right to small absorption at the left hand side. The derivative of the time-integrated probe beam transmission $T_E(x)$ with respect to the propagation direction x of the pump beam $(\partial T_E / \partial x)$

represents the temporal shape of the probe beam as will be shown below.

The pump beam excites molecules along its path. We approximate the population difference $N_1 - N_2$ by

$$N_1(x - tc/n) - N_2(x - tc/n)$$

$$= \Delta N + (N - \Delta N)\Theta(x - tc/n), \qquad (1)$$

N_1 and N_2 are the density of dye molecules in the ground state and excited state, respectively. $N = N_1 + N_2$ is the total density of molecules. ΔN is the residual population difference after the pump pulse has passed. Θ is the step function

$$\Theta(x - tc/n) = \begin{cases} 0 & \text{for } x - tc/n < 0 \\ 1 & \text{for } x - tc/n \geq 0 \end{cases} \qquad (2)$$

The situation is depicted in fig. 2a.

Assuming a constant intensity distribution of the pump beam across the width d of the dye sample one finds the following expression for the transverse transmission through the cell

$$T(x - tc/n) = \exp[-(N_1 - N_2)\sigma d]$$

$$= T_e(T_0/T_e)^{\Theta(x - tc/n)}, \qquad (3)$$

σ denotes the absorption cross-section of the dye. $T_0 = \exp[-N\sigma d]$ is the initial transmission, $T_e = \exp[-\Delta N\sigma d]$ represents the transmission of the bleached dye. The transmission is illustrated in fig. 2b.

The transverse probe pulse is expanded and focused with a cylindrical lens to the path of the pump beam. Along the cell length the probe profile should be constant, i.e. $I(t - zn/c, x) = I(t - zn/c)$. The incident intensity of the probe pulse is attenuated to a low value so that it does not change the population profile generated by the pump beam.

The time integrated transmission of the transverse beam through the sample is given by

$$T_E(x) = \int_{-\infty}^{\infty} I(t') \, T(x - tc/n) \, dt' \Big/ \int_{-\infty}^{\infty} I(t') dt' . \qquad (5)$$

$I(t')$ is the intensity of the incident probe beam ($z = 0$). The thickness d of the sample is neglected in eq. (5). The path lengths of the pump and probe pulse are adjusted that the peak of the probe pulse overlaps at x_0 with the transmission front. The time scales t and t' are therefore related by $t = t' + x_0 n/c$ and one finds (see fig. 2c)

$$T_E(x) = \frac{1}{E_{in}} \int_{-\infty}^{\infty} I(t') \, T_e(T_0/T_e)^{\Theta(x - x_0 - t'c/n)} \, dt'$$

$$= \frac{1}{E_{in}} \left[T_0 \int_{-\infty}^{(x-x_0)n/c} I(t') dt' \right.$$

$$\left. + T_e \int_{(x-x_0)n/c}^{\infty} I(t') dt' \right]. \qquad (6)$$

The abbreviation $E_{in} = \int_{-\infty}^{\infty} I(t') dt'$ was used in eq. (6). The derivative of $T_E(x)$ after x leads to

$$\frac{\partial T_E}{\partial x} = -\frac{(T_e - T_0)n}{E_{in}c} I\left(\frac{(x - x_0)n}{c}\right). \qquad (7)$$

The final result is (see fig. 2d)

$$I(t' = (x - x_0)n/c) = -\frac{E_{in}c}{(T_e - T_0)n} \frac{\partial T_E}{\partial x}. \qquad (8)$$

In the calculations presented above several approximations were used which are analysed now.

(i) The pump pulse does not generate an exact step function in the population difference and in the transverse transmission. In fig. 3 a real situation is considered. The population difference versus time is calculated at the entrance ($x = 0$) and inside the sam-
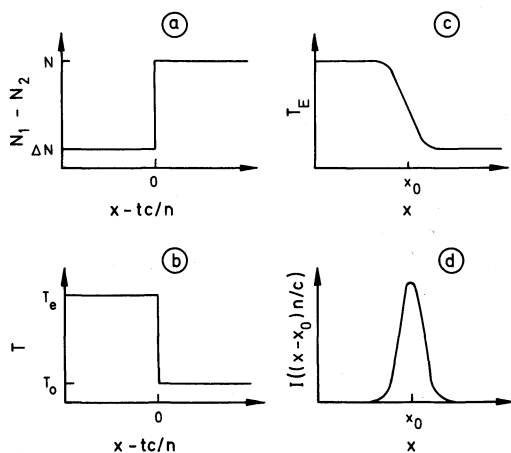
Fig. 2. Schematic representation of the relevant steps in pulse measurement. (a) Build-up of population difference in the sample caused by the pump pulse. (b) Change of intensity transmission transverse to the direction of the pump pulse. (c) Time integrated transmission $T_E(x)$ of the probe pulse along the propagation direction of the pump beam. (d) Temporal shape of probe pulse determined by $\partial T_E/\partial x$.
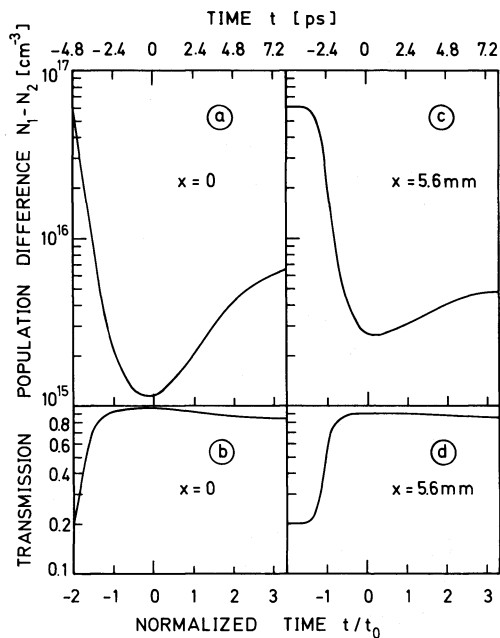
Fig. 3. Population differences and transverse transmission caused by a pump pulse in a dye sample at entrance ($x = 0$) and inside ($x = 5.6$ mm). Pump pulse parameters: peak intensity, $I_0 = 4 \times 10^{10}$ W/cm²; shape, gaussian $I_L = I_0 \exp[-(t/t_0)^2]$, duration $\Delta t_L = 4$ ps (fwhm). Dye: 10^{-4} M rhodamine 6G in ethanol. For the various parameters of the dye used in the calculation of the curves in (a) and (c) see refs. [13] and [14]. In (b) and (d) a small signal transmission of $T_0 = 0.2$ is assumed, corresponding to a transverse cell dimension of $d \approx 0.6$ mm.
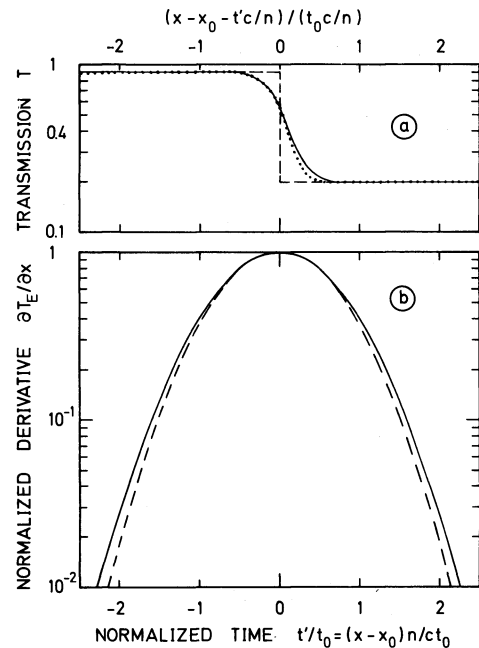

Fig. 4. Influence of transmission front on resolution of pulse shape. (a) Transmission profile. (b) Approximation of pulse shape by $\partial T_E/\partial x$. Dashed curves, step function (a) reproduces exactly the input pulse shape (b). Solid curve of (a) is given by eq. (9) and leads to solid curve of (b). Dotted line in (a) indicates the transmission determined by the situation of fig. 3d.

ple ($x = 5.6$ mm). A gaussian pulse with peak intensity $I_0 = 4 \times 10^{10}$ W/cm² and duration $\Delta t_L = 4$ ps (fwhm) is assumed to enter the cell filled with 10^{-4} M rhodamine 6G in ethanol (for the determination of the curves in fig. 3a and 3c see ref. [13]). At a cell thickness of $d \approx 0.6$ mm we find a small signal transmission of $T = 0.2$. The rise time of the transmission is about 1 ps.

The influence of the finite rise time on the time resolution is analysed in fig. 4. The shape of the input probe pulse is assumed to be gaussian ($I(t')/I_0 = \exp[-(t'/t_0)^2]$). The step function in fig. 4a reproduces the input pulse shape in fig. 4b (dashed curves). For smooth transmission fronts T the curves $\partial T_E/\partial x$ become broader than the temporal beam profiles $I(t')/I_0$. The solid curve in fig. 4a is given by

$$T = T_e + (T_0 - T_e)$$
$$\times \{ \tanh[4(x-x_0-t'c/n)/(t_0c/n)] + 1\}/2 . \quad (9)$$

($T_0 = 0.2$ and $T_e = 0.9$). It leads to the solid curve in fig. 4b. The broadening of $\partial T_E/\partial x$ is approximately 5 per cent compared to the step function. The dotted line of fig. 4a corresponds to fig. 3d and describes our experimental situation. It is well approximated by the solid curve and the finite rise of the transmission profile may be neglected.

(ii) The excited molecules relax to the ground state with a time constant τ. At high pump intensities and high dye concentrations the relaxation may be enhanced by amplified spontaneous emission [13,14] (see faster recovery time of $N_1 - N_2$ in fig. 3a compared to fig. 3c). The transverse transmission reduces with the relaxation of the excited molecules. Dyes with relaxation times $\tau \gg \Delta t_L$ should be used in the

measurements to avoid changes of T in the bleached region within the dureation of the probe beam $(T_e(x) = T_e)$. The situations depicted in figs. 3b and 3d fulfill this condition (note $\tau \approx 4.2$ ns for rhodamine 6G in ethanol).

(iii) The transmission front passes at a speed slightly slower than the light velocity c/n through the sample. The leading part of the pump pulse is absorbed until the molecules are excited. Figs. 3b and d show that the transmission front delays by about 2 ps over a distance of about 5 mm. The velocity of the transmission front is approximately $v \approx 0.9 \, c/n$. In eq. (8), $I(t' = (x - x_0)n/c)$ should be corrected by $I(t' = (x - x_0)/v) \approx I(t' = 1.1(x - x_0)n/c)$. The pulses are about 10% longer than indicated by the original form of eq. (8).

(iv) The measured pulse shape is averaged over the duration which the light needs to traverse the smaller of either the sample thickness of the pump beam diameter. The transverse dimension d determines the time resolution. For a thickness d we calculate a convolution time $t_c \approx dn/c$, and the pulse duration is approximately given by $\Delta t_L \approx (\Delta t_m^2 - t_c^2)^{1/2}$. Δt_m is the pulse duration measured by use of eq. (8). In most of our measurements we used $d \approx 0.4$ mm which implies $t_c \approx 2$ ps. Under our conditions the broadening of the pulse shape by finite sample width is compensated by the reduced propagation velocity of the transmission front. Good results were obtained by using the uncorrected form of eq. (8).

3. Experimental system

The experiments were carried out with a mode-locked Nd-phosphate glass laser system [15]. The mode-locking dye Eastman Nr. 9860 was used in a contacted dye cell. Single pulses were selected by use of an electro-optical shutter. The separated pulses were increased in energy with an amplifier. The energy of a single pulse behind the amplifier was approximately 5 mJ. Light pulses at the fundamental frequency ($\lambda_L = 1055$ nm), the second and the forth harmonic were investigated. The set-up for the pulse shape measurements is shown in fig. 5. A beam splitter BS separates the probe beam. The main beam serves as pump pulse. It is focused with lens L1 and its intensity at the sample was approximately 4 $\times$ 10^{10} W/cm^2. The beam diameter was ≈ 0.4 mm. A glass block in the absorber cell reduce the thickness
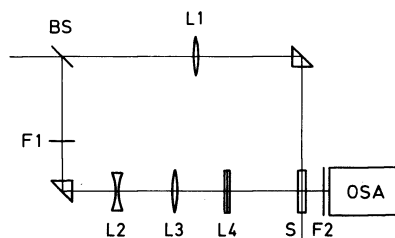
Fig. 5. Experimental set-up. BS, beam splitter; L1, lens ($f = 800$ mm in most experiments); S, cell with absorber, F1, filter to attenuate probe beam; L2 and L3, beam expander (magnification 8 in most cases); L4, cylindrical lens; F2, filter to discriminate fluorescence light; OSA, optical spectrum analyser.

Table 1

Laser wavelength (nm)	Absorber	Solvent	Concentration (M)	Absorption cross-section (cm^2)	Recovery time (ns)	Ref.
1055	Eastman 14015	1,2-dichloro-ethane	4 $\times 10^{-4}$	1 $\times 10^{-16}$	1	[17]
	Eastman 9860	1,2-dichloro-ethane	2 $\times 10^{-4}$	1.7 $\times 10^{-16}$	0.009	[19]
527.5	Rhodamine 6G	ethanol	1 $\times 10^{-4}$	4.2 $\times 10^{-16}$	4.2	[14]
352	Dimethyl POPOP	cyclohexane	1.5 $\times 10^{-4}$	1.8 $\times 10^{-16}$	1.5	[20]
264	9,10-dimethyl-anthracene	cyclohexane	1 $\times 10^{-4}$	2.8 $\times 10^{-16}$	6.1	[21,22]

of the dye solution to ca. 0.7 mm. The length of the cell was 2 cm. Proper dye solutions were selected for the various wavelengths of the light pulses (see table 1). The probe beam was attenuated with filters and expanded by an inverted telescope (lenses L2 and L3). The cylindrical lens L4 formed a line focus along the path of the pump beam. The path lengths of the pump and probe pulses were adjusted for temporal coincidence in the sample. The transmitted probe light was detected with a vidicon and processed with an optical spectrum analyser. Fluorescence light was filtered off with filters F2. The OSA data were transferred to a computer, where the data were corrected for variations of the incident probe beam across the sample length and the curves were smoothed [16], and differentiated.

4. Results

Pulse shape measurements were performed for various laser frequencies. The laser wavelengths and the applied dye solutions are listed in table 1.

(i) $\lambda = 1.055$ μm. The pulse shapes at the fundamental frequency of the Nd-glass laser were measured with the transition metal complex bis-(4-dimethyl-

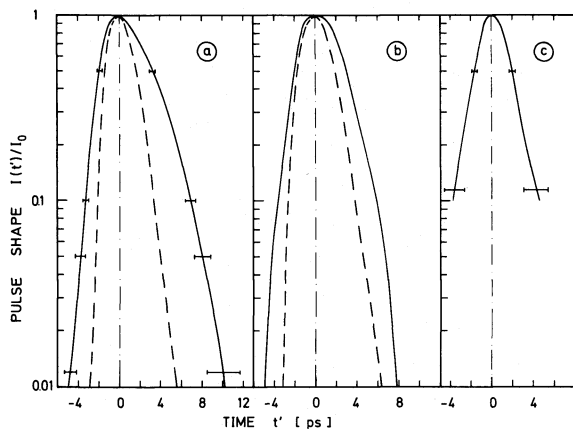Fig. 6. Examples of measured pulse shapes. (a) Picosecond light pulses at $\lambda = 1.055$ μm. Solid curve, unmodified pulse; $\Delta t_L = 5.5$ ps. Dashed curve, pulse shortened with saturable absorber; $\Delta t_L = 3.2$ ps. (b) Light pulses at $\lambda = 526.5$ nm. Solid curve, unchanged pulse; $\Delta t_L = 4.8$ ps. Dashed curve, pulse steepened by passage through rhodamine 6G solution; $\Delta t_L = 3.8$ ps. (c) Picosecond pulse at $\lambda = 264$ nm. $\Delta t_L = 3.6$ ps.

aminodithiobenzil)nickel (Eastman dye Nr. 14015) [17]. A typical pulse shape is shown by the solid curve in fig. 6a. Its duration is $\Delta t_L = 5.5$ ps. The shape is asymmetric; the leading edge is steeper than the trailing edge. This finding is in agreement with refs. [8] and [12]. The asymmetry is assumed to be due to the finite recovery time of the mode-locking dye. The pulse shape may be approximately fitted with a leading gaussian and a trailing secant hyperbolic $I(t) = I_0\{ (1 - \Theta(t)) \exp[-(t/t_0)^2] + \Theta(t)/\cosh^2[t/(\kappa t_0)]\}$ with $\kappa = 1.6 \pm 0.2$ (pulse duration $\Delta t_L = (0.83 + 0.88 \kappa)t_0$). The dashed curve in fig. 6a shows a probe pulse which was shortened by passing the probe beam through a saturable absorber (Eastman dye Nr. 9860 with small signal transmission $T_0 = 10^{-7}$, input intensity 6×10^9 W/cm^2). The pulse is shortened in good agreement with previous studies [18]. The pulse duration is $\Delta t_L = 3.2$ ps. The steep rise of the pulse indicates a high time resolution.

Pulse shape measurements with the saturable absorber Eastman Nr. 9860 [19] are possible but care has to be taken because of the fast recovery time ($\tau \approx 9$ ps).

(ii) $\lambda = 527.5$ nm. The dye rhodamine 6G was used at the second harmonic of the laser. In fig. 6b two temporal pulse profiles are shown. The solid curve shows the pulse shape of an unmodified second harmonic pulse. Its shape is similar to the solid curve of fig. 6a. The duration is $\Delta t_L = 4.8$ ps. The dashed curve was obtained by focussing the probe beam through a rhodamine 6G sample before entering the beam expander. The steepening of the leading edge should be noted.

(iii) $\lambda = 352$ nm. The dye dimethyl POPOP dissolved in cyclohexane may be used for pulse shape measurements at the third harmonic of the laser. It could be bleached with intense light pulses at $\lambda = 352$ nm.

(iv) $\lambda = 264$ nm. The pulse shapes at the fourth harmonic were investigated with 9,10-dimethyl anthracene dissolved in cyclohexane. Care has to be taken of two photon absorption of the solvent at high pump power intensities. Fig. 6c shows an example of the measured pulse shape. The duration is $\Delta t_L = 3.6$ ps.

It should be noted that at this wavelength in the ultraviolet the conventional techniques of TPF and SHG are not applicable.

5. Conclusions

The described method allows the determination of the temporal pulse profile to a high accuracy. The time resolution of the system may be adjusted to the duration of the probe pulse, i.e. for long probe pulses the beam diameter of the pump beam and the cell thickness may be increased and the dye concentration reduced. On the other hand, for short probe pulses small pump beam diameter and high dye concentration may be used. The probe beam may have weak energy content since sensitive vidicon detectors are available. The frequencies of the measured probe beam and the exciting pump beam may be different. The probe laser frequency should only be within the absorption band of the dye. The technique may be extended by monitoring the excited state absorption of the probe beam of convenient frequency after exciting the system with a pump beam.

Acknowledgements

References

[1] D.J. Bradley and G.H.C. New, Proc. IEEE 62 (1974) 313.
[2] P.W. Smith, M.A. Duguay and E.P. Ippen, Mode-Locking of lasers, Progress in Quantum Electronics, Vol. 3, Part 2 (Pergamon Press, 1974).
[3] E.P. Ippen and C.V. Shank, in: Ultrashort light pulses, ed. S.L. Shapiro, Topics in Appl. Phys., Vol. 18 (Springer-Verlag, Berlin, 1977) p. 83.
[4] J.A. Giordmaine, P.M. Rentzepis, S.L. Shapiro and K.W. Wecht, Appl. Phys. Lett. 11 (1967) 216.
[5] M. Maier, W. Kaiser and J.A. Giordmaine, Phys. Rev. Lett. 17 (1966) 1275.
[6] M.A. Duguay and J.W. Hansen, Appl. Phys. Lett. 15 (1969) 192.
[7] D.J. Bradley, B. Liddy, A.G. Roddie, W. Sibbett and W.E. Sleat, Optics Comm. 3 (1971) 426.
[8] D. von der Linde, A. Laubereau and W. Kaiser. Phys. Rev. Lett. 26 (1971) 954;
D. von der Linde and A. Laubereau, Optics Comm. 3 (1971) 279.
[9] D.H. Auston, Appl. Phys. Lett. 18 (1971) 249; Optics Comm. 3 (1971) 272.
[10] E.B. Treacy, Appl. Phys. Lett. 14 (1969) 112.
[11] J.W. Shelton and Y.R. Shen, Phys. Rev. Lett. 26 (1971) 538.
[12] G.R. Fleming, I.R. Harrowfield, A.E.W. Knight, J.M. Morris, R.J. Robbins and G.W. Robinson, Optics Comm. 20 (1977) 36.
[13] A. Penzkofer and W. Falkenstein, Opt. Quant. Electr. 10 (1978) 399.
[14] W. Falkenstein, A. Penzkofer and W. Kaiser, Optics Comm. 27 (1978) 151.
[15] A. Laubereau and W. Kaiser, Opto-Electr. 6 (1974) 1.
[16] P. Marchand and P. Veillette, Cand. J. Phys. 54 (1976) 1309.
[17] K.H. Drexhage and U.T. Müller-Westerhoff, IEEE J. Quant. Electr. QE-8 (1972) 759.
[18] A. Penzkofer, Opto-Electr. 6 (1974) 87.
[19] Eastman Kodak data release.
[20] I.B. Berlman, Handbook of fluorescence spectra of aromatic molecules (Academic Press, New York, 1966).
[21] DMS UV Atlas of organic compounds (Verlag Chemie, Weinheim, 1966).
[22] Landolt-Börnstein, New Series, Group II, Vol. 3: A. Schmillen and R. Legler, Luminescence of organic substances, eds. K.H. Hellwege and A.M. Hellwege (Springer-Verlag, Berlin, 1967).